PAPER

Check for updates

Lipofection with estrone-based luminophores featuring aggregation-induced emission properties†

Steffen Riebe,‡[a] Alexander Zimmermann,‡[a] Johannes Koch,[b] Cecilia Vallet,[c] Shirley K. Knauer,[c] Andrea Sowa,[a] Christoph Wölper[d] and Jens Voskuhl [ID] *[a]

In this communication we present the use of a novel class of luminophores with aggregation-induced emission (AIE) properties based on the steroid estrone. These molecules were equipped with cationic residues yielding amphiphiles suitable for lipofection. To this end, self-assembled luminescent structures were formed in aqueous media and mixed with a red-fluorescent protein expressing plasmid, yielding lipoplexes with increased emission intensity. These luminescent lipoplexes were able to efficiently transfect HeLa and HEK 293T cells and were able to be tracked due to the aggregation induced-emission properties.

The transport of genetic information into living cells yielding to hybridisation inside the nucleus is the key challenge in modern gene therapy. Over the past decades several approaches have been investigated to deliver specific DNA sequences and/or plasmids into nuclei to address severe diseases such as cancer[1–3] or neurodegenerative diseases such as Parkinson's[4,5] or Alzheimer's.[6,7] A major problem in this regard is the negative surface charge of the cellular corona based on the so-called glycocalyx, which mainly consists of sialic acids and its derivatives.[8] This prevents the entering of genetic information due to strong electrostatic repulsion of the phosphate backbones and the cellular surface. To this end, several approaches have been investigated to overcome this major problem. Three different compound classes have been used to form neutral to cationic complexes with DNA sequences: (A) small cationic organic compounds and cationic polymers, (B) cationic amphiphiles[9,10] and (C) retroviruses,[11] which are able to cross the membrane barrier and induce efficient transfection. All these potential candidates have their individual advantages and disadvantages. Small organic cationic compounds or polymers[12–14] (*e.g.*

polyethyleneimine, PEI) are known to be toxic at higher doses, which also is the case of amphiphilic structures such as Lipofectamine 2000™.[15] Retroviruses are known to induce an immune response to the infected body leading to severe side effects.[16,17] Especially lipofection has attracted our interest since the formation of larger self-assembled structures bearing multiple cationic charges at their surface leads to efficient DNA carriers (lipoplex). Here, several approaches for the use of amphiphiles to generate vesicles,[18] micelles[19] and nanotubes[20] have been described in literature. Lehn[21] and Huang *et al.*[22] showed that the variation of the hydrophobic tail (*e.g.* cholesterol) had a huge influence on the transfection ability of cationic amphiphiles. Besides the variation of the hydrophobic part also the cationic head groups have been varied extensively. Here, especially linear or branched amines[23] and oligoamines[24] and oligoarginines[25,26] as well as artificial binding motifs such as guanidinium–carbonylpyrroles[27–29] have attracted interest and were able to efficiently induce transfection.

Up to now, the exact mode of action (*e.g.* the pathway of the vectors through the cell membrane and inside the cytosol) remained unclear in most of the above mentioned examples. Thus, we decided to use the well-known AIE-effect to follow the way of transfection. Here, luminophores show induced emission when fixed in a steric demanding (*e.g.* in the aggregated, bound or solid state) environment due to a restriction of intramolecular motion. First AIE-active compounds were described by Tang *et al.* back in 2001. Recently, we were able to synthesize a novel and easily accessible class of AIE emitters with fluorescence and phosphorescence properties. These compounds were already used for numerous applications such as luminescent micelles,[30] organogels,[31,32] liquid crystals[33,34] and bio-imaging.[35] Here, we combine our unique system with the

[a]Institute for Organic Chemistry and CENIDE, University of Duisburg-Essen, Universitätsstrasse 7, 45141 Essen, Germany. E-mail: jens.voskuhl@uni-due.de

[b]ICCE, Center of Medical Biotechnology (ZMB), University of Duisburg-Essen, Universitätsstrasse 2, 45141 Essen, Germany

[c]Department of Molecular Biology II, Center of Medical Biotechnology (ZMB), University of Duisburg-Essen, 45117 Essen, Germany

[d]Institute for Inorganic Chemistry and Center for NanoIntegration (CENIDE), University of Duisburg-Essen, Universitätsstrasse 5–7, 45117 Essen, Germany
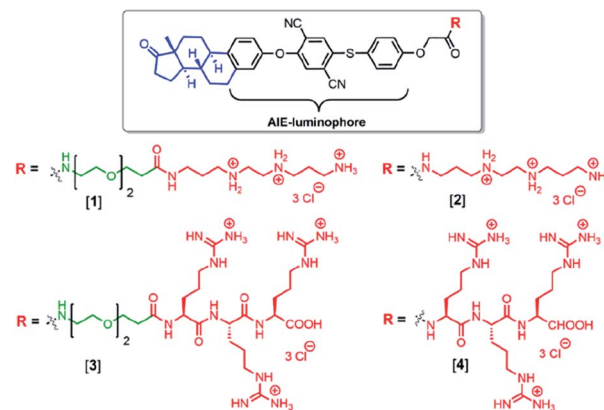
† Electronic supplementary information (ESI) available: For synthesis, photophysical properties, characterisation of the formed structures and CLSM-microscopy. CCDC 1938010. For ESI and crystallographic data in CIF or other electronic format see DOI: 10.1039/d0ra03608k

‡ These authors contributed equally.

steroid estrone, conveying luminescence properties due to its aromatic unit. Furthermore estrone was used, since it bears the characteristic steroid backbone, which is also existent in cholesterol, which is a vital part of the cellular membrane. Hence we assume a strong interaction of our transfection vectors with the cellular membrane, leading to an efficient uptake. Moreover, it is essential to mediate interactions with the cellular membrane *via* cationic groups such as oligoamines or tri-arginines. Subsequently, the obtained amphiphiles are able to assemble into higher ordered structures. These supra-structures should allow electrostatically binding of DNA sequences or plasmids leading to lipoplexes, which will be tested for their transfection capacity (Scheme 1). Furthermore, the self-assembled structures will be fluorescent due to the restriction of motion of the AIE active core motif upon self-assembly. Besides that, increased emission is expected upon DNA (mRFP-plasmid) binding due to cross linking of the single higher ordered structures. This behaviour furthermore enables the tracking of the lipoplexes inside the cellular environment. A further advantage of this design is the role of the luminophore as vital part – the hydrophobic residue in the amphiphile – of the transfection system, compared to the classic labelling approach of known vectors, which is often accompanied by enhanced toxicity (Scheme 2).[36,37]

Compounds [1] and [2] were synthesized by coupling tri-(boc) protected *N,N'*-bis(2-aminoethyl)-1,3-propanediamine to the carboxylic acid functionalized compounds [F] (Fig. 1) and the triethyleneglycol containing analogues [H] followed by acid-assisted deprotection (see ESI†). The synthesis for compounds [3] and [4] started from a solid phase synthesis assisted route. Three arginines were coupled on the resin followed by attachment of either the AIE luminophore [F] or the AIE active compound with triethyleneglycol spacer [H] under peptide coupling conditions (see ESI†). The structure of [F] was confirmed by X-ray crystallography (see ESI†). [F] crystallizes in the tetragonal space group $P4_12_12$ with one molecule plus a DMF solvent molecule in the asymmetric unit. Alternatively,
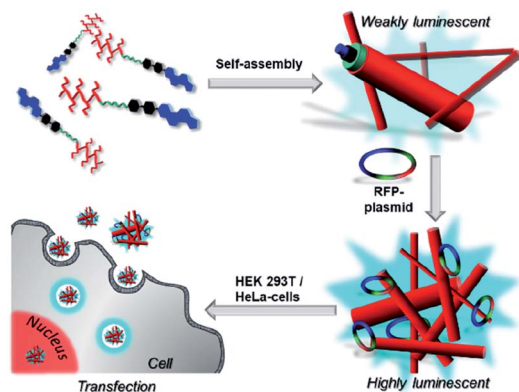
a description as merohedral twin in space group $P4_1$ is possible (Fig. 1 and S17†).

From the obtained data it can be seen that all bond lengths and angles are within the expected range and the overall conformation of the estrone residue remains unchanged.

With these compounds in stock we performed an in depth investigation of the self-assembly properties of all four compounds in water in the presence and absence of plasmid, expressing a fluorescent protein (RFP), C-terminally fused to a nuclear histone protein H2B (pH2B-mRFP).

Compounds [1–4] were dissolved in water followed by vor-texing, yielding self-assembled structures which were investi-gated by fluorescence spectroscopy (Fig. S10†).

Here in all cases an emission signal at around 470–480 nm was observed which can be excited at 380 nm (see Fig. S9†), due to the formation of self-assembled structures in aqueous media. This emission cannot be observed in DMSO due to the free molecular movement, which is typical for aggregation-induced emission. The critical aggregation concentration (CAC) was determined by dilution of the aqueous samples followed by tracking of the emission wavelength, assuming a change in emission upon self-assembly due to changes in the molecular environment. Here, in all cases a change in the emission wavelength was determined for concentrations below 2 μM (Fig. S14 and S15†). To get a deeper impression of the morphology of compounds [1–4] in aqueous media, TEM imaging was performed (Fig. 2D, E and S16†). Compound [1] and [2], both revealed fibre-like structures with a thickness of around 10–15 nm, whereas [3] and [4] showed more granular and less organized morphologies in aqueous media (Fig. S16†).

Scheme 2 Molecular structures of the estrone-based AIE-active transfection vectors used in this study.

Scheme 1 Self-assembly of AIE active amphiphiles followed by the formation of luminescent lipoplexes in the presence of plasmid DNA as well their ability to transfect cells. The schematic presentation is not to scale.
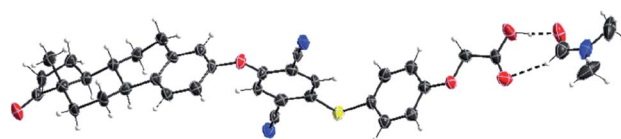

Fig. 1 X-ray structure of [F] × 1 DMF. Displacement ellipsoids are drawn at 50% probability levels.
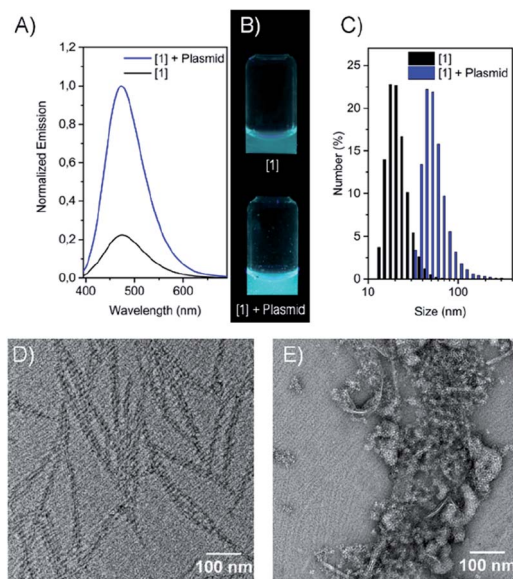
Fig. 2 (A) Emission of compound [1] as pure sample and in the presence of the mRFP plasmid, (B) photographs of [1] as pure sample and in the presence of the mRFP plasmid under UV-light irradiation ($\lambda = 365$ nm), (C) DLS spectra of [1] and [1] in the presence of the pH2B-mRFP plasmid, c[1] = 100 μM, c(pH2B-mRFP plasmid) = 10 μg mL^{-1} (D) TEM images of [1] and (E) [1] in the presence of RFP plasmid. c[1] = 500 μM, c(pH2B-mRFP plasmid) = 50 μg mL^{-1}.

Fig. 4 Concentration-dependent cytotoxicity as determined by an MTS assay of compounds [1–4] compared with lipofectamine™ 2000 as reference.

These structures showed low to moderate emission properties, which was attributed to a higher polarity and a weaker packing inside the aggregates (Fig. S10 and S12†). Besides that, ζ-potential measurements showed highly positively charged assemblies with a potential between 42–62 mV as expected for the cationic amphiphiles. Next, the influence of electrostatic binding of the RFP-plasmid was investigated in detail. The morphologies obtained were mixed with the plasmid and emission wavelengths, sizes, ζ-potentials as well as the morphologies were determined. Interestingly, in all cases
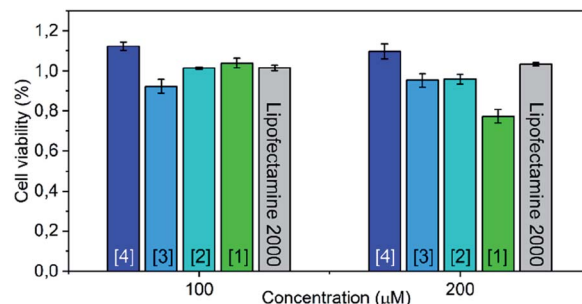
a drastic fluorescence increase was observed due to the assumed formation of densely packed lipoplexes, hindering additionally the motion of the estrone-based AIE core (Fig. 2B, S12, and S13†). Besides that, for most of the compounds an increased size was determined by DLS-measurements attributed to the formation of larger structures (Fig. 2C and S6†). The decrease in ζ-potential for the lipoplexes goes along with the partial charge neutralisation (e.g. for [1] without plasmid = 62 mV and with plasmid = 49 mV) (Fig. S7 and S8†). Here compound [3] showed only marginal changes in the ζ-potential which was explained by a weak or incomplete accessibility of the cationic head groups for the plasmid DNA. TEM imaging revealed larger aggregates (lipoplexes) showing in the case of [1] (Fig. 2E) and [2] networks of thin fibres in close contact, whereas [3] and [4] showed crosslinked assemblies with worm-like morphologies (Fig. S16†). After confirmation of the electrostatically assembled lipoplexes with enhanced emission properties, first experiments to use these structures for transfection of HeLa and HEK 293T cells were conducted in which we tested the ability of the compounds [1–4] to transport plasmid DNA into cell. Therefore, HeLa und HEK 293T cells were incubated with a solution of the compounds pre-mixed with plasmid DNA.
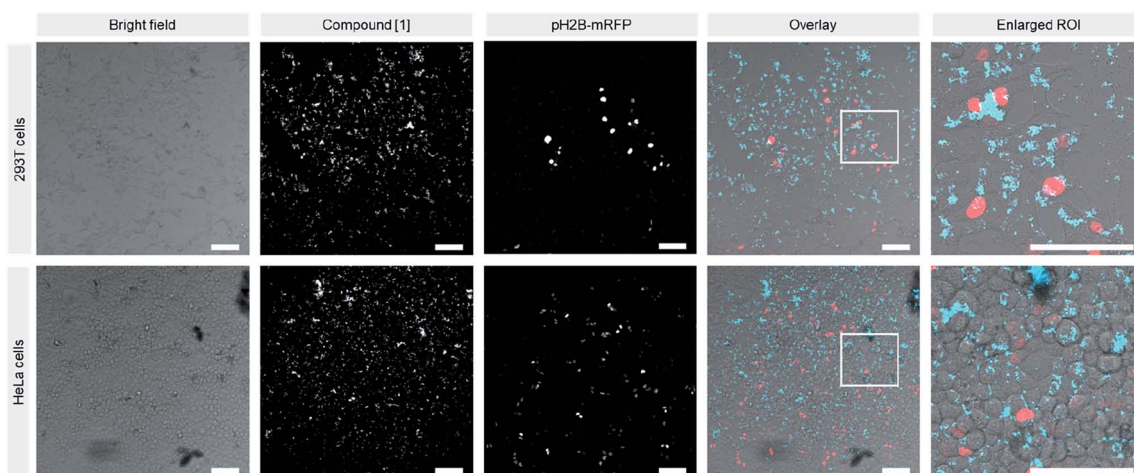

Fig. 3 Confocal images of HEK 293T (upper panels) and HeLa cells (lower panels) 16 h after transfection of pH2B-mRFP (red) with [1]. Scale bar: 100 μm (concentrations: [1] = 48 μM, pH2B-mRFP plasmid = 2.4 μg mL^{-1}).

After 16 h these cells were analyzed *via* confocal laser scanning microscopy. Surprisingly only for compounds [1] and [2] nuclear RFP was observed, which is indicative for successful gene delivery (Fig. 3 and S20–S22†). However transfection efficiency was only marginal for [2], and treatment of cells with this compound resulted in an abnormal morphology even at low concentrations (10 μM). Compounds [3] and [4] were not able to mediate gene transfection (Fig. S23 and S24†). Thus, we focused our research on the transfection properties of [1].

The lipoplex of [1] and pH2B-mRFP was uniformly taken up by both cell lines and led to an efficient transfection rate inferior to Lipofectamine™ 2000 (Fig. S18, S19, and S26†).

The determined transfection efficiency of compound [1] in comparison with the gold standard Lipofectamine™ 2000 was determined. In the case of HEK 293T cells an efficiency of 8.4% and for HeLa cells 12.6% was found which is lower than Lipofectamine™ 2000 (31.4% (HeLa), 31.6% (HEK 293T)) (Fig. S26†).

In contrast to Lipofectamine™, localization of the lipoplex can easily be monitored by the AIE-effect of the estrone based luminophore (Fig. 3 and S18–S20†). To assess the cytotoxicity of the compounds, we performed an MTS assay, which showed a slightly decreased viability of HeLa cells treated with [1] at high concentrations compared to Lipofectamine™ 2000-treated cells (Fig. 4). Interestingly, compound [1] seemed to localize in spherical vesicles within the cells after transfection. To clarify the mechanism of uptake, we treated HeLa cells with [1] pre-mixed with plasmid DNA and stained the lysosomes with LysoTracker™ Green (Fig. S25†). We observed a partial colocalization of [1] with the lysosomes, which suggests an uptake *via* the endosomal pathway followed by an endosomal escape or lysosomal degradation. Although we are aware that the transfection potential of our compound so far is still inferior to the gold standard of lipofection, it opens a completely new field of transfections vectors featuring AIE-properties. These are enabling future research by varying the single parts of the vectors, *e.g.* cationic headgroups, linker as well as steroid anchors. Furthermore, we were able to show that the AIE luminophore is not only a luminescent tag but also key structure of the transfection system representing a completely novel approach for transfection vectors.

Conflicts of interest

There are no conflicts to declare.

Acknowledgements

Notes and references

1 F. McCormick, *Nat. Rev. Cancer*, 2001, **1**, 130.

2 A. El-Aneed, *J. Controlled Release*, 2004, **94**, 1–14.

3 R. G. Vile, S. J. Russell and N. R. Lemoine, *Gene Ther.*, 2000, **7**, 2.

4 M. G. Kaplitt, A. Feigin, C. Tang, H. L. Fitzsimons, P. Mattis, P. A. Lawlor, R. J. Bland, D. Young, K. Strybing, D. Eidelberg and M. J. During, *Lancet*, 2007, **369**, 2097–2105.

5 P. A. LeWitt, A. R. Rezai, M. A. Leehey, S. G. Ojemann, A. W. Flaherty, E. N. Eskandar, S. K. Kostyk, K. Thomas, A. Sarkar, M. S. Siddiqui, S. B. Tatter, J. M. Schwalb, K. L. Poston, J. M. Henderson, R. M. Kurlan, I. H. Richard, L. Van Meter, C. V. Sapan, M. J. During, M. G. Kaplitt and A. Feigin, *Lancet Neurol.*, 2011, **10**, 309–319.

6 M. H. Tuszynski, L. Thal, M. Pay, D. P. Salmon, H. S. U, R. Bakay, P. Patel, A. Blesch, H. L. Vahlsing, G. Ho, G. Tong, S. G. Potkin, J. Fallon, L. Hansen, E. J. Mufson, J. H. Kordower, C. Gall and J. Conner, *Nat. Med.*, 2005, **11**, 551.

7 M. H. Tuszynski, *Alzheimer Dis. Assoc. Disord.*, 2007, **21**, 179–189.

8 N. M. Varki and A. Varki, *Lab. Invest.*, 2007, **87**, 851.

9 J. Zabner, A. J. Fasbender, T. Moninger, K. A. Poellinger and M. J. Welsh, *J. Biol. Chem.*, 1995, **270**, 18997–19007.

10 H. Farhood, N. Serbina and L. Huang, *Biochim. Biophys. Acta, Biomembr.*, 1995, **1235**, 289–295.

11 W. S. Pear, G. P. Nolan, M. L. Scott and D. Baltimore, *Proc. Natl. Acad. Sci. U. S. A.*, 1993, **90**, 8392–8396.

12 D. G. Anderson, D. M. Lynn and R. Langer, *Angew. Chem.*, 2003, **115**, 3261–3266.

13 H. Lv, S. Zhang, B. Wang, S. Cui and J. Yan, *J. Controlled Release*, 2006, **114**, 100–109.

14 D. Fischer, T. Bieber, Y. Li, H.-P. Elsässer and T. Kissel, *Pharm. Res.*, 1999, **16**, 1273–1279.

15 A. Masotti, G. Mossa, C. Cametti, G. Ortaggi, A. Bianco, N. D. Grosso, D. Malizia and C. Esposito, *Colloids Surf., B*, 2009, **68**, 136–144.

16 M. Mesri, N. R. Wall, J. Li, R. W. Kim and D. C. Altieri, *J. Clin. Invest.*, 2001, **108**, 981–990.

17 E. Check, *Nature*, 2003, **423**, 573.

18 S. Oguchi, M. Kamihira, J. You, A. Tachibana and S. Iijima, *J. Ferment. Bioeng.*, 1998, **86**, 118–120.

19 C. Wölk, D. Pawlowska, S. Drescher, A. Auerswald, A. Meister, G. Hause, A. Blume, A. Langner, G. Brezesinski and B. Dobner, *Langmuir*, 2014, **30**, 4905–4915.

20 A. K. Salem, P. C. Searson and K. W. Leong, *Nat. Mater.*, 2003, **2**, 668.

21 J. P. Vigneron, N. Oudrhiri, M. Fauquet, L. Vergely, J. C. Bradley, M. Basseville, P. Lehn and J. M. Lehn, *Proc. Natl. Acad. Sci. U. S. A.*, 1996, **93**, 9682–9686.

22 X. Gao and L. Huang, *Biochem. Biophys. Res. Commun.*, 1991, **179**, 280–285.

23 S. Fletcher, A. Ahmad, E. Perouzel, M. R. Jorgensen and A. D. Miller, *Org. Biomol. Chem.*, 2006, **4**, 196–199.

24 S. Fletcher, A. Ahmad, W. S. Price, M. R. Jorgensen and A. D. Miller, *ChemBioChem*, 2008, **9**, 455–463.

25 V. B. Morris and C. P. Sharma, *Biomaterials*, 2010, **31**, 8759–8769.

26 N. A. Alhakamy and C. J. Berkland, *Mol. Pharmaceutics*, 2013, **10**, 1940–1948.

27 K. Samanta, P. Jana, S. Bäcker, S. Knauer and C. Schmuck, *Chem. Commun.*, 2016, **52**, 12446–12449.

28 X.-Y. Hu, M. Ehlers, T. Wang, E. Zellermann, S. Mosel, H. Jiang, J.-E. Ostwaldt, S. K. Knauer, L. Wang and C. Schmuck, *Chem.–Eur. J.*, 2018, **24**, 9754–9759.

29 P. Jana, K. Samanta, S. Bäcker, E. Zellermann, S. Knauer and C. Schmuck, *Angew. Chem.*, 2017, **129**, 8195–8200.

30 P. Ahlers, C. Götz, S. Riebe, M. Zirbes, M. Jochem, D. Spitzer, J. Voskuhl, T. Basché and P. Besenius, *Polym. Chem.*, 2019, **10**, 3163–3169.

31 D. Aschmann, S. Riebe, T. Neumann, D. Killa, J.-E. Ostwaldt, C. Wölper, C. Schmuck and J. Voskuhl, *Soft Matter*, 2019, **15**, 7117–7121.

32 M. Externbrink, S. Riebe, C. Schmuck and J. Voskuhl, *Soft Matter*, 2018, **14**, 6166–6170.

33 S. Riebe, M. Saccone, J. Stelzer, A. Sowa, C. Wolper, K. Soloviova, C. A. Strassert, M. Giese and J. Voskuhl, *Chem.–Asian J.*, 2019, **14**, 814–820.

34 M. Saccone, M. Blanke, C. G. Daniliuc, H. Rekola, J. Stelzer, A. Priimagi, J. Voskuhl and M. Giese, *ACS Mater. Lett.*, 2019, **1**, 589–593.

35 J. Stelzer, C. Vallet, A. Sowa, D. Gonzalez-Abradelo, S. Riebe, C. G. Daniliuc, M. Ehlers, C. A. Strassert, S. K. Knauer and J. Voskuhl, *ChemistrySelect*, 2018, **3**, 985–991.

36 R. S. Gupta and A. K. Dudani, *J. Cell. Physiol.*, 1987, **130**, 321–327.

37 J. S. Modica-Napolitano and J. R. Aprille, *Cancer Res.*, 1987, **47**, 4361–4365.